Transformation of methyl laurate into lauryl alcohol over a Ru-Sn-Mo/C catalyst by using zerovalent iron and water as an in situ hydrogen source

Sagata, Kunimasa
Hirose, Mina
Hirano, Yoshiaki
Kita, Yuichi

(Citation)
Applied Catalysis A: General,523:85-91

(Issue Date)
2016-08-05

(Resource Type)
journal article

(Version)
Accepted Manuscript

(URL)
https://hdl.handle.net/20.500.14094/90003555

Submitted to Applied Catalysis A: General *as a research article*

Transformation of methyl laurate into lauryl alcohol over a Ru–Sn–Mo/C catalyst by using zerovalent iron and water as an in situ hydrogen source

Kunimasa SAGATA, Mina HIROSE, Yoshiaki HIRANO, and Yuichi KITA*

Department of Chemical Science and Engineering, Graduate School of Engineering, Kobe University, Kobe 657-8501, Japan

* Corresponding author

Yuichi KITA: Department of Chemical Science and Engineering,
Graduate School of Engineering,
Kobe University, Kobe 657-8501, Japan.
Tel. +81-78-803-6244
Fax +81-78-803-6512
E-mail: yuichi_kita@lion.kobe-u.ac.jp

Abstract

Hydrogenation and hydrogenolysis reactions, which are used in the chemical industry for the synthesis of organic compounds, are very expensive operations because of the need for facilities that can liquefy, transport, and store the hydrogen produced through steam reforming of natural gas. We have therefore developed a novel approach for hydrogenation that does not require the use of high-cost facilities. Using this, zerovalent iron (Fe) and water (H_2O) are introduced as an in situ hydrogen donor system for the transformation of methyl laurate into lauryl alcohol over a Ru-based catalyst. This combination of a Ru–Sn–Mo/C catalyst with a Fe/H_2O system showed significantly higher transformation rates for the conversion of methyl laurate into lauryl alcohol than a conventional reaction system that uses pressurized hydrogen. The reason for this is that the new system produces lauric acid as an intermediate during the reaction, which is more efficiently hydrogenized into lauryl alcohol over the Ru–Sn–Mo/C catalyst. The Fe/H_2O system played two important roles: a hydrogen source for the hydrogenation reaction and a catalyst for the generation of lauric acid by methyl laurate hydrolysis.

Keywords: Zerovalent iron; Hydrogenation; Hydrolysis; Methyl laurate; Ru catalyst

1. Introduction

Hydrogen (H_2) is an important chemical feedstock and emerging energy carrier that is typically produced from hydrocarbon fuels through steam reforming, partial oxidation, or autothermal reforming. Industrial production of H_2 is predominantly dependent on the steam reforming of methane, the economic viability of which is adversely affected as the scale of a production plant is decreased [1]. Large plants for hydrogen production are therefore necessary to ensure the most cost-effective operations. Additionally, as hydrogen gas needs to be converted into compressed H_2 gas or liquid H_2 for transportation and storage purposes, its use can be quite expensive. Indeed, it can cost in excess of 200 million US dollars to carry out the comprehensive processes of H_2 liquefaction (51 tons d^{-1}, 75 million US dollars), transportation (12,000 m^3/ship, 82 million US dollars), and storage (3000 m^3 $plant^{-1}$, 54 million US dollars) [2]. Given these costs, any method that could allow reduction reactions such as hydrogenation and hydrogenolysis to proceed without the use of expensive hydrogen would be highly desirable.

Hydrogenation and hydrogenolysis reactions are hugely significant catalytic reactions that are used in the laboratory and chemical industry for organic synthesis. Recently, biomass resources, particularly unused biomass such as agricultural residues

and forest offcuts, have garnered significant attention as sustainable and renewable raw materials for the production of chemicals [3–5]. However, the viability of converting biomass resources into valuable chemicals via hydrogenation and hydrogenolysis reactions depends on their location characteristics with regards to the scale and ease of biomass feedstock procurement, hydrogen production and storage capacities, and product transfer networks. New catalytic procedures that have been explored for hydrogenation and hydrogenolysis in the absence of any added hydrogen include: aqueous phase reforming (e.g., $C_3H_8O_3$ (glycerol) + $3H_2O \rightarrow 3CO_2 + 7H_2$) [6–9], catalytic transfer hydrogenation (e.g., C_3H_8O (2-propanol) → C_3H_6O (acetone) + H_2) [10–12], and water gas shift reactions ($CO + H_2O = CO_2 + H_2$) [13–15] in which the supply of hydrogen comes from an in situ source.

It is well known that hydrogen can be produced by chemically reacting metals and metal oxides such as Fe [16–18], Zn [19,20], W [17], FeO [21], MnO [22], SnO [23], and Ce_2O_3 [24] with steam at elevated temperatures. Hydrogenation reactions that employ a reaction between metals (Al, Fe, Mn, and Zn) and water have also been investigated for the reduction of many organic and inorganic compounds such as nitroarenes [25,26], aryl chlorides [27,28], aldehydes [29], biomass-derived glycolides [30], bio-oil [31], and carbon dioxide [32,33]. To regenerate oxidized metals and metal

oxides, the following processes have been proposed as renewable energy sources: reducing gases from biomass gasification [34], biomass-derived char [35,36], and solar thermal energy [31,37]. Thus, metal/metal-oxide water systems used as in situ hydrogen donors can potentially be used for eco-friendly chemical synthesis via hydrogenation and hydrogenolysis reactions. The zerovalent iron (Fe) and water (H_2O) system is particularly valuable in this regard, because Fe is an abundant and cheap resource that can be used to produce H_2 in accordance with reactions (1) and (2):

$$\mathrm{Fe(s)} + \mathrm{H_2O(g)} \rightarrow \mathrm{FeO(s)} + \mathrm{H_2(g)} \quad (1)$$

$$\mathrm{3FeO(s)} + \mathrm{H_2O(g)} \rightarrow \mathrm{Fe_3O_4(s)} + \mathrm{H_2(g)} \quad (2)$$

Here, (s) and (g) represent solids and gases, respectively. The use of H_2 derived from nanoscale Fe and H_2O has been investigated for removing contaminants such as *p*-nitrophenol [38], trichloroethylene [39], hexachlorobenzene [40], and 4-chlorophenol [41] from water via catalytic hydrogenation; however, it has not yet been applied to the production of useful chemicals.

Fatty alcohols derived from renewable resources such as vegetable oils are an industrially important feedstock for the synthesis of surfactants and plasticizers. Fatty

alcohols are produced by the hydrogenation of fatty acid esters, which are obtained by transesterification of triglycerides using methanol or fatty acids from the hydrolysis of fats [42]. During the hydrogenation of fatty acids and esters, copper–chromite-based catalysts are commonly used at high temperatures (250–300 °C) and pressures (20–30 MPa). To date, a large number of heterogeneous catalysts have been investigated based on noble metals (Ru [43–47], Rh [48], and Pt [49]) or transition metals (Cu [9,50] and Co [51–53]), and have been shown to exhibit high activity under mild conditions.

In this work, we employed Fe and H_2O (Fe/H_2O) as an in situ hydrogen donor for the transformation of methyl laurate into lauryl alcohol over a Ru–Sn–Mo/C catalyst. The performance of Ru–Sn–Mo/C with this Fe/H_2O system was compared to a conventional reaction system that uses pressurized hydrogen.

2. Experimental

2.1. Catalyst preparation

The Ru–Sn–Mo/C catalyst was prepared by a conventional impregnation method using aqueous solutions of $RuCl_3 \cdot nH_2O$ (41.1%, Ru content, Wako Pure Chemical Industries, Ltd.), $SnCl_4 \cdot 5H_2O$ (100.1%, Wako Pure Chemical Industries, Ltd.), and $(NH_4)_6Mo_7O_{24} \cdot 4H_2O$ (100.7%, Wako Pure Chemical Industries, Ltd.) with activated

charcoal (Sigma-Aldrich, Norit SX Ultra). Typically, 316 mg of $RuCl_3 \cdot nH_2O$, 222 mg of $SnCl_4 \cdot 5H_2O$, and 23 mg of $(NH_4)_6Mo_7O_{24} \cdot 4H_2O$ were placed into an evaporating dish, and 2 g of ultrapure water was added to dissolve the salts. After adding 857 mg of activated charcoal, the mixture was dried in a water bath at 90 °C while stirring. The resulting impregnated catalyst was vacuum-dried overnight at 70 °C and the resulting catalyst was reduced at 350 °C for 1 h under hydrogen (99.999%) at a flow rate of 50 $cm^3 \cdot min^{-1}$.

Oxidized-Fe sample was prepared from 60–80 nm Fe particles (99.9%, 1564 mg, product number: NM-0029-UP, Ionic Liquids Technologies), H_2O (1 g), and tetradecane (99.7%, 40 mL, Wako Pure Chemical Industries, Ltd.) in a 100 mL Hastelloy C high-pressure reactor (OM Lab-Tech, MMJ-100). For this, the reactor was first purged four times with nitrogen, and then heated to 270 °C and held at this temperature for 24 h at a stirring rate of 1000 rpm. After cooling to room temperature, the oxidized iron was separated by filtration, washed with acetone, and then vacuum-dried overnight at 70 °C.

2.2. Characterization

To determine the crystalline phase of the catalyst, X-ray powder diffraction (XRD) analyses were performed using a Rigaku SmartLab diffractometer with CuKα radiation. X-ray fluorescence (XRF) analyses were also performed to determine composition of

the fresh and spent catalyst using a Rigaku ZSX Primus II apparatus with RhKα radiation. A Brunauer–Emmett–Teller (BET) analysis was conducted to determine the specific surface area of the catalyst; this was accomplished by using N_2 adsorption at -196 °C with a BEL Japan Bellsorp-mini II instrument. The surface chemical states of the Ru–Sn–Mo/C were evaluated by X-ray photoelectron spectroscopy (XPS) analyses (JPS-9000MX, JEOL) with a MgKα excitation source. All binding energy values in the XPS spectra were referenced to the C 1s line at 285.0 eV.

Temperature programmed desorption (NH_3-TPD and CO_2-TPD) experiments were carried out in a flow apparatus with helium as the carrier gas using a MicrotracBEL BELCAT-A. Prior to these experiments, the samples (0.2 g) were pretreated for 1 h at 300 °C under He (30 $cm^3 \cdot min^{-1}$) to remove the adsorbate. Once the samples were cooled to 100 °C, probe molecules (9.79% NH_3/He or 5.02% CO_2/He) were introduced into the reactor until their concentration in the effluent gas was unchanged. The samples were subsequently flushed at the same temperature for 1 h to remove any physically adsorbed probe molecules, then heated to 700–750 °C at heating rates of 10 $°C \cdot min^{-1}$ under helium flow (30 $cm^3 \cdot min^{-1}$). Any desorbed NH_3 or CO_2 gas was detected by a quadrupole mass spectrometer.

2.3. Hydrogenation of methyl laurate

Methyl laurate (99.4%, 870 mg, Wako Pure Chemical Industries, Ltd.), Ru–Sn–Mo/C catalyst (43 mg), Fe (28 mmol (1564 mg) of 60–80nm particles without previous activation), H_2O (28–83 mmol), and tetradecane were introduced into a 100 mL Hastelloy C high pressure reactor. After purging the reactor four times with nitrogen, it was heated to the required temperature and maintained at that state for 1–24 h. The stirring rate was adjusted to 1000 rpm. The resulting products were separated by centrifugation and filtration, and their yields were determined by gas chromatography on an instrument equipped with a flame ionization detector (Shimadzu, GC-2014) using anisole as an internal standard. A capillary column (Restek, Stabilwax) was used to analyze the esters, alcohols, acids, and higher molecular weight hydrocarbons. The conversion of methyl laurate and yield of product were defined as follows:

$$\text{Conversion (\%)} = \frac{n_{Methyl\ laurate,0} - n_{Methyl\ laurate}}{n_{Methyl\ laurate,0}} \times 100 \quad (3)$$

$$\text{Yield (\%)} = \frac{n_{Product}}{n_{Methyl\ laurate,0}} \times 100 \quad (4)$$

Here, $n_{Methyl\ laurate,0}$ is the initial molar amount of methyl laurate, $n_{Methyl\ laurate}$ represents the molar amount of methyl laurate in the reaction system at the end of the reaction, and

$n_{Product}$ indicates the molar amount of the particular product. The material balance based on the C12 unit was 100 ± 7% during the transformation of methyl laurate into lauryl alcohol. Decomposition reactions such as the hydrogenolysis of tetradecane solvent were not observed under the reaction conditions tested.

3. Results and discussion

3.1. Characterization of Ru-Sn-Mo/C

Information for the Ru–Sn–Mo/C catalyst is listed in Table 1. Note that XPS measurement of the reduced Ru–Sn–Mo/C was conducted after exposure to air. The binding energy of Ru 3p3/2 was 462.7 eV, and this value could be ascribed to anhydrous RuO_2 in accordance with the values reported for this species [54–56]. The binding energies of Sn were 484.7 and 487.1 eV for Sn $3d_{5/2}$, suggesting the presence of Sn^0 [57] and Sn^{4+} [58], respectively. Binding energies for Mo 3d5/2 were observed at 229.2, 232.5, and 236.0 eV, suggesting the presence of MoO_2 [59] and MoO_3 [60], respectively.

No detectable diffraction lines for ruthenium-, tin- or molybdenum-related crystallites species were observed in XRD measurements of the Ru–Sn–Mo/C catalyst, which suggests that these species can only exist as fine particles below the detectable level of

XRD (< 10 nm).

3.2. H_2 generation behavior of the Fe/H_2O system

Figure 1 shows the H_2 pressure observed from the Fe/H_2O system at 270 °C over time. It was confirmed from gas chromatography-thermal conductivity detector (GC-TCD) measurements that the gaseous product generated was hydrogen. In this study, a hydrogen pressure of ca. 1.8 MPa was equivalent to approximately 36 mmol of hydrogen (where the theoretical amount in the Fe and H_2O reaction is $3Fe + 4H_2O \rightarrow Fe_3O_4 + 4H_2$). When the reactor was immediately cooled to room temperature after reaching 270 °C, the observed H_2 pressure was 0.4 MPa. A H_2 pressure of 0.6 MPa was achieved after 8 h, after which no further increase in pressure was observed at the end of 24 h. The observed H_2 pressure derived from the Fe/H_2O system was unchanged in the presence of Ru–Sn–MoOx/C (data not shown here).

3.3. Transformation of methyl laurate over Ru–Sn–Mo/C with the Fe/H_2O system

The transformation of methyl laurate into lauryl alcohol over the Ru–Sn–Mo/C catalyst with the Fe/H_2O system proving an in situ H_2 source was compared to the transformation achieved using a conventional reaction system with pressurized H_2.

Figure 2 shows the time needed for the transformation of methyl laurate over the Ru–Sn–Mo/C catalyst with pressurized H_2 and the Fe/H_2O system. The detected products consisted of lauryl alcohol, lauric acid, lauryl laurate, undecane, and dodecane, with similar products having been previously observed in the hydrodeoxygenation of methyl laurate on silica-supported Ni-Mo phosphides [61]. The proposed reaction pathway is presented in Scheme 1. Here, methyl laurate is transformed to lauric acid via hydrogenolysis or hydrolysis, and then successively converted to lauryl alcohol by the hydrogenation of lauryl aldehyde via the hydrogenolysis of lauric acid. Lauryl laurate is generated by the esterification of lauric acid and lauryl alcohol, which is an ester-exchange reaction that occurs very easily without a catalyst [48]. Undecane is formed by the hydrogenation of undecene via the decarbonylation of lauryl aldehyde, while dodecane is produced by the hydrogenation of dodecene via the dehydration of lauryl alcohol.

In the catalytic system with pressurized H_2, the lauryl alcohol yield increased almost linearly over a period of 8 h, but increased only gradually thereafter for a gain of 39% at the end of 24 h. Moreover, the lauryl laurate yield gradually increased with increasing reaction time. Conversely, in the catalytic system with Fe/H_2O, the lauryl alcohol yield increased with respect to time for a gain of 61% at the end of 24 h. The yield of lauric

acid also increased from 6% at 1 h to 30% at 8 h. Any further reaction, however, led to a decline in the lauric acid yield. The lauryl laurate yield, on the other hand, gradually increased with time. These results demonstrate that when used with the Fe/H_2O system, the Ru–Sn–Mo/C catalyst can efficiently hydrogenize methyl laurate during the production of lauryl alcohol, much unlike the pressurized-H_2 system. However, as shown in Fig. 1, the H_2 pressure achieved with the Fe/H_2O system (0.6 MPa) was lower than that for the conventional pressurized-H_2 system (1.0 MPa). Given that the hydrogenation of fatty acid esters generally requires a high H_2 pressure for the production of fatty alcohols [42], it is presumed that the use of Ru–Sn–Mo/C with a pressurized-H_2 system will need a higher H_2 pressure to achieve methyl laurate conversion and lauryl alcohol yields equivalent to those from the use of Ru–Sn–Mo/C with the Fe/H_2O system. Reaction rates for the transformation of methyl laurate to lauryl alcohol at 15% methyl laurate conversion and turnover frequencies (TOF) based on the total Ru metal were calculated to be 50 mmol·$g_{Ru.}^{-1}$·h^{-1} and 5 h^{-1}, respectively, with pressurized H_2, and 76 mmol· $g_{Ru.}^{-1}$·h^{-1} and 8 h^{-1} with the Fe/H_2O system.

Transformation of methyl laurate over the Ru–Sn–Mo/C catalyst with the Fe/H_2O system was performed for varying water contents in the H_2O/Fe molar ratio range of 1−3. Figure 3 (a) shows the effect of the molar ratio of H_2O to Fe on the transformation

of methyl laurate and the amount of H_2 generated. When the molar ratio was increased from 1 to 2, the yield of lauryl alcohol increased from 50 to 61%, the reason for which was the increase in the amount of H_2 generated as the H_2O/Fe ratio was increased (Fig. 3). However, increases in the molar ratio from 2 to 3 decreased the lauryl alcohol yield from 61 to 34%, even though the amount of H_2 generated was large. A similar phenomenon was observed in the catalytic system with pressurized H_2 (Fig. 3 (b)). That is, when the H_2O content was increased from 0 to 56 mmol, the lauryl alcohol yield increased from 40 to 53%. Further increases in H_2O addition from 56 to 83 mmol significantly decreased the lauryl alcohol yield from 53 to 14%, while greatly increasing the lauric acid yield. While the reasons why the lauryl alcohol yield was decreased by the high H_2O/Fe molar ratio remain unclear, there is a possible explanation for this phenomenon that involves a change in the active phase. That is, an increase in the by-product (undecane) yield is indicative of a change in active phase during effective lauryl alcohol production in the case of H_2O/Fe = 3. Indeed Table 2 confirms that the Sn/Ru atomic ratio in spent Ru–Sn–Mo/C with H_2O/Fe = 3 was lower than the Sn/Ru ratio with H_2O/Fe ≤ 2. In the present reaction system, the amount of saturated water vapor at 270 °C is calculated to be ca. 60 mmol. Consequently, all of the H_2O in the case of H_2O/Fe ≤ 2 (H_2O ≤ 56 mmol) exists as steam at the reaction temperature used,

whereas a portion of the H_2O in the case of H_2O/Fe = 3 (H_2O = 83 mmol) exists as condensed water in addition to steam. This presence of condensed water might have caused an accelerated change in the active phase through leaching.

3.4. Roles of the Fe/H_2O system during the transformation of methyl laurate

Herein, we investigate the influence of the Fe/H_2O system on the transformation of methyl laurate into lauryl alcohol over a Ru–Sn–Mo/C catalyst. XRD analysis was performed to examine the changes in crystalline phase during the hydrogenation reaction. The XRD diffraction patterns obtained are shown in Fig. 4. The fresh Fe samples provided a strong diffraction line at 44.7° that was assigned to Fe^0 (Joint Committee on Powder Diffraction Standards (JCPDS) file No. 6-0696), as well as broad lines at 30.1°, 35.5°, and 43.1° that were assigned to Fe_3O_4 (JCPDS file No. 19-629). A decrease in the intensity of the diffraction line of Fe^0 was observed after the reaction, whereas the intensity of the Fe_3O_4 peaks increased. Thus, Fe with H_2O largely converted the crystalline phase to Fe_3O_4 during the reaction as follows: $3Fe + 4H_2O \rightarrow Fe_3O_4 + 4H_2$. However, as previously reported in the literature [62], this Fe/H_2O system may also produce various types of solid iron such as FeO, Fe_2O_3, and FeOOH in addition to Fe_3O_4.

To verify that the use of the Ru–Sn–Mo/C catalyst with the Fe/H_2O system resulted in the production of lauric acid during the reaction presented above, methyl laurate was treated under Fe/H_2O and oxidized-Fe/H_2O in the absence of Ru–Sn–Mo/C (Table 3). Both the Fe/H_2O and oxidized-Fe/H_2O reaction systems achieved effective conversion of methyl laurate to lauric acid compared with Ru-Sn-Mo/C + H_2O system, whereas a blank test without Fe exhibited only trace amounts of lauric acid. It is well known that acidic and basic catalysts in the presence of water lead to the hydrolysis of fatty acid methyl esters [63], and so NH_3- and CO_2-TPD measurements were conducted to investigate the acid–base properties of oxidized-Fe samples after reaction in the absence of Ru–Sn–Mo/C and a methyl laurate substrate. In the NH_3- and CO_2-TPD profiles of the oxidized-Fe sample shown in Figure 5, NH_3 desorption peaks were observed in the temperature range of 120–270 °C and 280–400 °C. This suggests that the oxidized-Fe sample contained weak acidic sites [64]. In the CO_2-TPD profile of the oxidized-Fe sample, on the other hand, at least two kinds of CO_2 desorption peaks were detected. One was observed in the temperature range of 250–400 °C and the other was observed in the temperature range of 500–730 °C. According to the literature [65,66], the lower temperature peaks may be assigned to CO_2 adsorbed on weak basic sites, while the peaks at higher temperatures may be assigned to CO_2 adsorbed on strong basic sites.

These results lead to the assumption that Ru–Sn–Mo/C with the Fe/H_2O system produced lauric acid by hydrolysis over acid–base sites of Fe species.

The hydrogenation reactivity of lauric acid as an intermediate during the transformation of methyl laurate to lauryl alcohol was compared with that of methyl laurate. In the results listed in Table 4, it is evident that the catalytic system with pressurized H_2 achieved almost complete conversion of lauric acid, and that the yields of lauryl alcohol for lauric acid were higher than those for methyl laurate. In the case of a lauric acid substrate, the lauryl alcohol yields and product distributions were similar in both catalytic systems. These results indicate that the hydrogenation of lauric acid is faster than that of methyl laurate, and that the Fe/H_2O system does not have a particular effect in the hydrogenation of lauric acid.

Taking the above experimental results into consideration, the influence of the Fe/H_2O system on the transformation of methyl laurate over the Ru–Sn–Mo/C catalyst was considered. In addition to the Ru–Sn–Mo/C catalyst, the Fe/H_2O system produced a large amount of lauric acid through the hydrolysis of methyl laurate over Fe species such as Fe_3O_4. This lauric acid was efficiently reduced into lauryl alcohol over the Ru–Sn–Mo/C catalyst via the in situ hydrogen generated from the Fe/H_2O reaction, which resulted in a high lauryl alcohol yield.

As can be seen in the experimental results, in addition to not requiring expensive H_2 facilities for liquefaction, transportation and storage, our Ru–Sn–Mo/C catalyst with the Fe/H_2O system has been proven to be useful for the transformation of methyl laurate into lauryl alcohol. Clearly, in order to further develop this Fe/H_2O system for hydrogenation and hydrogenolysis reactions, we need to conduct further studies. In particular, it would be useful to investigate the reusability of Fe, identify those iron materials most suitable for highly efficient hydrogen generation, improve the reaction system in terms of its hydrogen utilization efficiency, and determine the applicability of this Fe/H_2O system to other hydrogenation reactions. Work is also currently underway to investigate the possibility of magnetically separating the oxidized-iron and hydrogenation catalyst, with the aim of creating an economical and sustainable process in which the oxidized-iron is regenerated using biomass waste, and the resulting reducing gas is used to regenerate the hydrogenation catalyst. If successful, we hope that this Fe/H_2O reaction system can blaze a new path toward the realization of economical hydrogenation and hydrogenolysis reaction systems.

4. Conclusions

We attempted to employ zerovalent iron (Fe) and water (H_2O) as an in situ hydrogen

source for the transformation of methyl laurate into lauryl alcohol. The transformation of methyl laurate over the Ru–Sn–Mo/C catalyst with this Fe/H_2O system resulted in a highly efficient transformation of methyl laurate into lauryl alcohol when compared with conventional reaction systems that employ pressurized hydrogen. During reaction, Ru–Sn–Mo/C with Fe/H_2O produced lauric acid as an intermediate, which was easily hydrogenized into lauryl alcohol by the Ru–Sn–Mo/C catalyst. The results obtained suggest that the Fe/H_2O system serves two important functions during the highly efficient transformation of methyl laurate into lauryl alcohol over the Ru–Sn–Mo/C catalyst. The first is to provide a hydrogen source for the hydrogenation reaction, while the second is as a catalyst for the generation of lauric acid by methyl laurate hydrolysis.

Acknowledgements

This work was supported by the Japan Society for the Promotion of Science (JSPS) KAKENHI program (Grant-in-Aid for Exploratory Research, Grant Number 26620147) and the Nippon Shokubai Co., Ltd.

References

[1] S. Galera, F.J. Gutierrez Ortiz, Fuel 144 (2015) 307–316.

[2] T. Watanabe, K. Murata, S. Kamiya, K. Sakata, Y. Ishimoto, J. Jpn. Soc. Energy Resour. 31 (2010) 24–31.

[3] M. Besson, P. Gallezot, C. Pinel, Chem. Rev. 114 (2014) 1827–1870.

[4] A. Corma, S. Iborra, A. Velty, Chem. Rev. 107 (2007) 2411–2502.

[5] J.N. Chheda, G.W. Huber, J.A. Dumesic, Angew. Chem. Int. Ed. 46 (2007) 7164–7183.

[6] R.D. Cortright, R.R. Davda, J.A. Dumesic, Nature 418 (2002) 964–967.

[7] J.D. Holladay, J. Hu, D.L. King, Y. Wang, Catal. Today 139 (2009) 244–260.

[8] G. W. Huber, J. A. Dumesic, Catal. Today 111 (2006) 119–132.

[9] S. Liang, H. Liu, J. Liu, W. Wang, T. Jiang, Z. Zhang, B. Han, Pure Appl. Chem. 84 (2012) 779–788.

[10] G. Brieger, T.J. Nestrick, Chem. Rev. 74 (1974) 567–580.

[11] J. Jae, W. Zheng, R.F. Lobo, D.G. Vlachos, Chemsuschem 6 (2013) 1158–1162.

[12] A. Shrotri, H. Kobayashi, A. Tanksale, A. Fukuoka, J. Beltramini, Chemcatchem 6 (2014) 1349–1356.

[13] L. He, L.C. Wang, H. Sun, J. Ni, Y. Cao, H.Y. He, K.N. Ean, Angew. Chem. Int. Ed.

48 (2009) 9538–9541.

[14] A. Tlili, J. Schranck, H. Neumann, M. Beller, Chem. Eur. J. 18 (2012) 15935–15939.

[15] L. Yu, X.L. Du, J. Yuan, Y.M. Liu, Y. Cao, H.Y. He, K.N. Fan, Chemsuschem 6 (2013) 42–46.

[16] V. Hacker, R. Fankhauser, G. Faleschini, H. Fuchs, K. Friedrich, M. Muhr, K. Kordesch, J. Power Sources 86 (2000) 531–535.

[17] M. Thaler, V. Hacker, Int. J. Hydrogen Energy 37 (2012) 2800–2806.

[18] E. Lorente, Q. Cai, J.A. Pena, J. Herguido, N.P. Brandon, Int. J. Hydrogen Energy 34 (2009) 5554–5562.

[19] A. Steinfeld, Int. J. Hydrogen Energy 27 (2002) 611–619.

[20] K. Wegner, H.C. Ly, R.J. Weiss, S.E. Pratsinis, A. Steinfeld, Int. J. Hydrogen Energy 31 (2006) 55–61.

[21] P. Charvin, S. Abanades, G. Flamant, F. Lemort, Energy 32 (2007) 1124–1133.

[22] P. B. Kreider, H. H. Funke, K. Cuche, M. Schmidt, A. Steinfeld, A. W. Weimer, Int. J. Hydrogen Energy 36 (2011) 7028–7037.

[23] S. Abanades, Int. J. Hydrogen Energy 37 (2012) 8223–8231.

[24] W.C. Chueh, S.M. Haile, Philos. Trans. R. Soc. A 368 (2010) 3269–3294.

[25] C. Boix, N. Poliakoff, J. Chem. Soc. Perkin Trans. 1 11 (1999) 1487–1490.

[26] L. Wang, P.H. Li, ZT. Wu, J.C. Yan, M. Wang, Y.B. Ding, Synthesis-Stuttgart 13 (2003) 2001–2004.

[27] S. Mukhopadhyay, G. Rothenberg, D. Gitis, M. Baidossi, D.E. Ponde, Y. Sasson, J. Chem. Soc. Perkin Trans. 2 9 (2000) 1809–1812.

[28] S. Mukhopadhyay, G. Rothenberg, D. Gitis, Y. Sasson, Org. Lett. 2 (2000) 211–214.

[29] S. Mukhopadhyay, G. Rothenberg, H. Wiener, Y. Sasson, New J. Chem. 24 (2000) 305–308.

[30] L. Xu, Z. Huo, J. Fu, F. Jin, Chem. Commun. 50 (2014) 6009–6012.

[31] C. Hargus, R. Michalsky, A.A. Peterson, Energy Environ. Sci. 7 (2014) 3122–3134.

[32] F. Jin, Y. Gao, Y. Jin, Y. Zhang, J. Cao, Z. Wei, R. L. Smith, Jr., Energy Environ. Sci. 4 (2011) 881–884.

[33] X. Zeng, M. Hatakeyama, K. Ogata, J. Liu, Y. Wang, Q. Gao, K. Fujii, M. Fujihira, F. Jin, S. Nakamura, Phys. Chem. Chem. Phys. 16 (2014) 19836–19840.

[34] F. Li, L. Zeng, L.S. Fan, Fuel 89 (2010) 3773–3784.

[35] Y. Cao, B. Casenas, W.P. Pan, Energy Fuels 20 (2006) 1845–1854.

[36] H. Leion, E. Jerndal, B.M. Steenari, S. Hermansson, M. Israelsson, E. Jansson, M.

Johnsson, R. Thunberg, A. Vadenbo, T. Mattisson, A. Lyngfelt, Fuel 88 (2009) 1945–1954.

[37] P. Krenzke, K. Krueger, N. Leonard, S. Duncan, R.D. Palumbo, S. Möller, *J. Sol. Energy Eng.*, 132 (2010) 034501.

[38] B. Lai, Y. Zhang, Z. Chen, P. Yang, Y. Zhou, J. Wang, Appl. Catal. B 144 (2014) 816–830.

[39] W. Yan, A.A. Herzing, X.Q. Li, C.J. Kiely, W.X. Zhang, Environ. Sci. Technol. 44 (2010) 4288–4294.

[40] X. Nie, J. Liu, X. Zeng, D. Yue, J. Environ. Sci. 25 (2013) 473–478.

[41] F. Xu, S. Deng, J. Xu, W. Zhang, M. Wu, B. Wang, J. Huang, G. Yu, Environ. Sci. Technol. 46 (2012) 4576–4582.

[42] T. Turek, D.L. Trimm, Catal. Rev. Sci. Eng. 36 (1994) 645–683.

[43] S. Taniguchi, T. Makino, H. Watanuki, Y.U. Kojima, M. Sano, T. Miyake, Appl. Catal. A 397 (2011) 171–173.

[44] V.M. Deshpande, K. Ramnarayan, C.S. Narasimhan, J. Catal. 121 (1990) 174–182.

[45] Y. Pouilloux, F. Autin, C. Guimon, J. Barrault, J. Catal. 176 (1998) 215–224.

[46] Y. Pouilloux, A. Piccirilli, J. Barrault, J. Mol. Catal. A: Chem. 108 (1996) 161–166.

[47] M.A. Sánchez, Y. Pouilloux, V.A. Mazzieri, C.L. Piec, Appl. Catal. A 467

(2013) 552–558.

[48] T. Miyake, T. Makino, S.I. Taniguchi, H. Watanuki, T. Niki, S. Shimizu, Y. Kojima, M. Sano, Appl. Catal. A 364 (2009) 108–112.

[49] K.I. Gursahani, R. Alcala, R.D. Cortright, J.A. Dumesic, Appl. Catal. A 222 (2001) 369–392.

[50] H. Huang, G. Cao, C. Fan, S. Wang, S. Wang, Korean J. Chem. Eng. 26 (2009) 1574–1579.

[51] K.D.O. Vigier, Y. Pouilloux, J. Barrault, Catal. Today 195 (2012) 71–75.

[52] Y. Pouilloux, F. Autin, A. Piccirilli, C. Guimon, J. Barrault, Appl. Catal. A 169 (1998) 65–75.

[53] Q. Liu, Y. Bie, S. Qiu, Q. Zhang, J. Sainio, T. Wang, L. Ma, J. Lehtonen, Appl. Catal. B 147 (2014) 236–245.

[54] B. Yang, Q. Lu, Y. Wang, L. Zhuang, P. Liu, J. Wang, R. Wang, Chem. Mater. 15 (2003) 3552–3557.

[55] R. Chetty, W. Xia, S. Kundu, M. Bron, T. Reinecke, W. Schuhmann, M. Muh-ler, Langmuir 25 (2009) 3853–3860.

[56] J.H. Ma, Y.Y. Feng, J. Yu, D. Zhao, A.J. Wang, B.Q. Xu, J. Catal. 275 (2010) 34–44.

[57] J.C. Serrano-Ruiz, G.W. Huber, M.A. Sánchez-Castillo, J.A. Dumesic, F. Rodríguez-Reinoso, A. Sepúlveda-Escribano, J. Catal. 241 (2006) 378–388.

[58] M. del C. Aguirre, P. Reyes, M. Oportus, I. Melián-Cabrera, J.L.G. Fierro, Appl. Catal. A 233 (2002) 183–196.

[59] P. A. Spevack, N.S. Mcintyre, J. Phys. Chem. 96 (1992) 9029–9035.

[60] H. Al-Kandari, F. Al-Kharafi, N. Al-Awadi, O.M. El-Dusouqui, S.A. Ali, A. Katrib, Appl. Catal. A 295 (2005) 1–10.

[61] J. Chen, Y. Yang, H. Si, M. Li, Y. Chu, Z. Pan, X. Yu, Fuel 129 (2014) 1–10.

[62] C. Noubactep, Environ. Technol. 29 (2008) 909–920.

[63] S. Yan, S.O. Salley, K. Y.S. Ng, Appl. Catal. A 353 (2009) 203–212.

[64] J. Han, D. Zhang, P. Maitarad, L. Shi, S. Cai, H. Li, L. Huang, J. Zhang, Catal. Sci. Technol. 5 (2015) 438–446.

[65] K. Sagata, N. Imazu, H. Yahiro, Catal. Today 201 (2013) 145–150.

[66] L. Li, L. Song, H. Wang, C. Chen, Y. She, Y. Zhan, X. Lin, Q. Zheng, Int. J. Hydrogen Energy 36 (2011) 8839–8849.

Table 1. Properties of the Ru–Sn–Mo/C catalyst.

Loading / %			Atomic ratio / −		Binding energy / eV			S_{BET} [a]	V_{pore} [b]	D_{pore} [c]
Ru	Sn	Mo	Sn/Ru	Mo/Ru	Ru	Sn	Mo	/ $m^2 \cdot g^{-1}$	/ $cm^3 \cdot g^{-1}$	/ nm
6.1	2.9	1.0	0.40	0.18	462.7	487.1	229.2	591	0.59	4.0
						487.7	232.5			
							236.0			

[a]BET surface area, [b]Pore volume, and [c]Pore diameter.

Table 2. Sn/Ru and Mo/Ru atomic ratio of spent Ru-Sn-Mo/C.

H_2O/Fe	Atomic ratio / −	
molar ratio / −	Sn/Ru	Mo/Ru
1	0.39	0.16
2	0.43	0.15
3	0.31	0.14

Table 3. Hydrolysis of methyl laurate in an Fe/H_2O system.

Entry	Reaction system	Conversion / %	Product yield / %	
			Lauryl aldehyde	Lauric acid
1	Fe/H_2O[1)]	49	9	40
2	Oxidized-Fe/H_2O[2)]	67	−	62
3	Ru-Sn-Mo/C + H_2O[3)]	21	−	16
4	H_2O	< 1	−	< 1

Reaction conditions; Methyl laurate = 4 mmol, [1)]Fe = 28 mmol, [2)]Fe_3O_4 = 9.3 mmol, [3)]Ru-Sn-Mo/C = 43 mg, H_2O = 56 mmol, Tetradecane = 40 mL, Pressure = N_2 0.1 MPa, Temperature = 270 °C, and Time = 24 h.

Table 4. Hydrogenation of methyl laurate and lauric acid over a Ru–Sn–Mo/C catalyst using pressurized H_2 and the Fe/H_2O system.

Entry	Reaction system	Substrate	Conversion / %	Product yield / %				
				Lauryl alcohol	Lauric acid	Lauryl laurate	Undecane	Dodecane
1	Ru–Sn–Mo/C + H_2	Methyl laurate[1)]	67	40	−	14	5	2
2	Ru–Sn–Mo/C + H_2	Lauric acid[2)]	> 99	60	< 1	31	3	2
3	Ru–Sn–Mo/C + Fe/H_2O	Lauric acid[3)]	98	58	2	28	3	4

Reaction conditions; [1)]Methyl laurate = 4 mmol, [2)]Lauric acid = 4 mmol, Ru–Sn–Mo/C = 43 mg, Tetradecane = 40 mL, Pressure = H_2 1.0 MPa, Temperature = 270 °C, and Time = 24 h. [3)]Lauric acid = 4 mmol, Fe = 28 mmol, H_2O = 56 mmol, Tetradecane = 40 mL, Ru-Sn-Mo/C = 43 mg, Pressure = N_2 0.1 MPa, Temperature = 270 ^{o}C, and Time = 24 h.

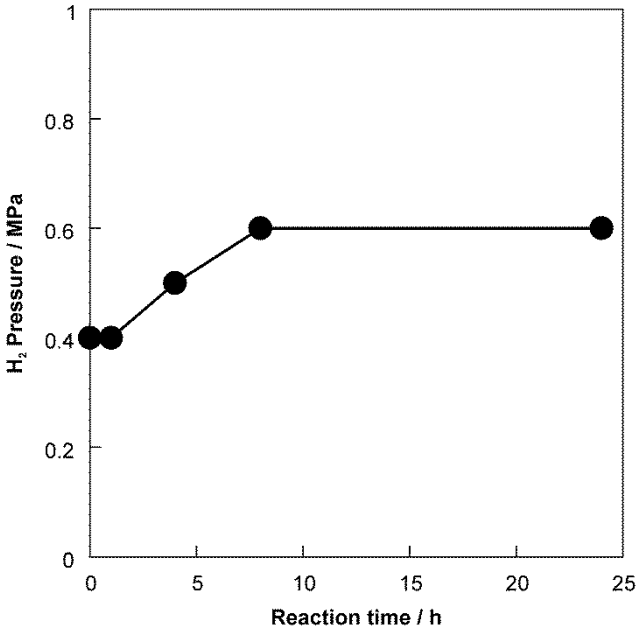

Fig. 1. Observed variation in H_2 pressure of Fe/H_2O system as a function of time at 270 °C. Reaction conditions; Fe = 28 mmol, H_2O = 56 mmol, Tetradecane = 40 mL, Pressure = N_2 1.0 MPa, Temperature = 270 °C, and Time = 0–24 h.

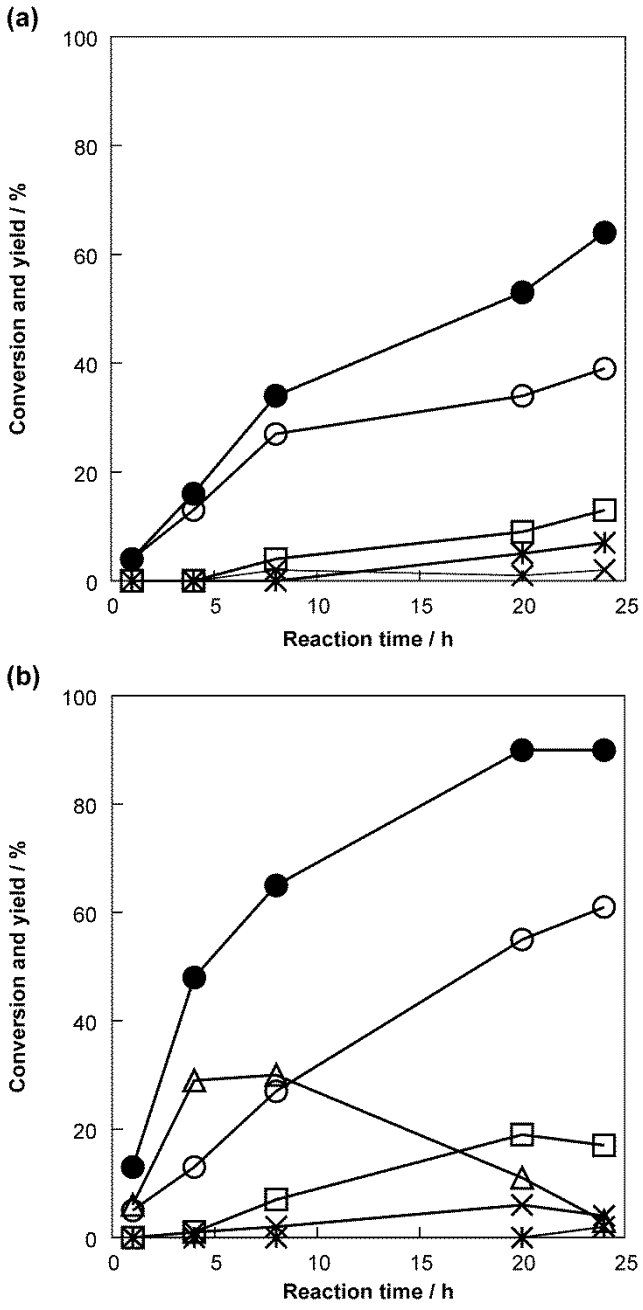

Fig. 2. Time for hydrogenation of methyl laurate over a Ru–Sn–Mo/C catalyst with (a) pressurized H_2 and (b) the Fe/H_2O system. (●) Conversion, (○) lauryl alcohol, (Δ) lauric acid, (□) lauryl laurate, (x) undecane, and (*) dodecane. Reaction conditions; (a) Methyl

laurate = 4 mmol, Ru–Sn–Mo/C = 43 mg, Tetradecane = 40 mL, Pressure = H_2 1.0 MPa, Temperature = 270 °C, and Time = 24 h. (b) Methyl laurate = 4 mmol, Ru–Sn–Mo/C = 43 mg, Fe = 28 mmol, H_2O = 56 mmol, Tetradecane = 40 mL, Pressure = N_2 1.0 MPa, Temperature = 270 °C, and Time = 24 h.

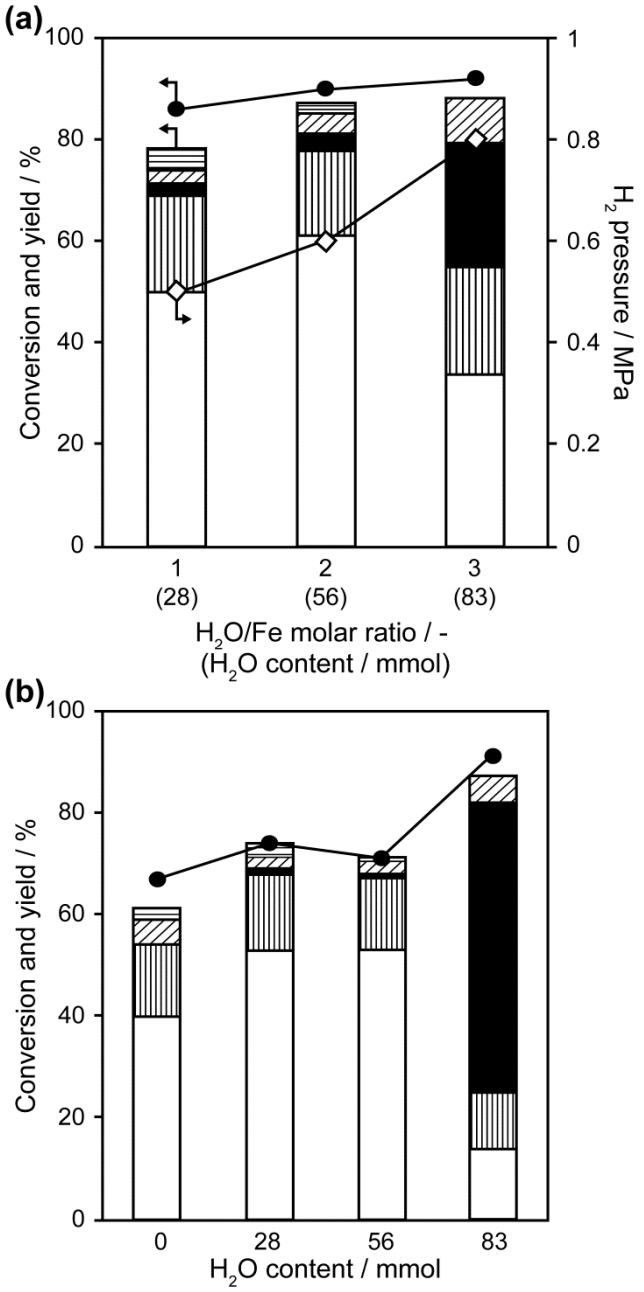

Fig. 3 Effect of H_2O/Fe ratio on the catalytic activity of a Ru–Sn–Mo/C catalyst with (a) the Fe/H_2O system and (b) pressurized H_2. (●) Conversion, (white bar) lauryl alcohol, (vertical bar) lauryl laurate, (black bar) lauric acid, (diagonal bar) undecane, (horizontal bar) dodecane, and (◊) observed H_2 pressure from the Fe/H_2O system at 270 °C for 24 h

in the absence of methyl laurate and Ru–Sn–Mo/C. Reaction conditions; (a) Methyl laurate = 4 mmol, Ru–Sn–Mo/C = 43 mg, Fe = 28 mmol, H_2O = 28–83 mmol, Tetradecane = 40 mL, P_{N2} = 1.0 MPa, Temperature = 270 °C, and Time = 24 h. (b) Methyl laurate = 4 mmol, Ru–Sn–Mo/C = 43 mg, H_2O = 0–83 mmol, Tetradecane = 40 mL, Pressure = H_2 1.0 MPa, Temperature = 270 °C, and Time = 24 h.

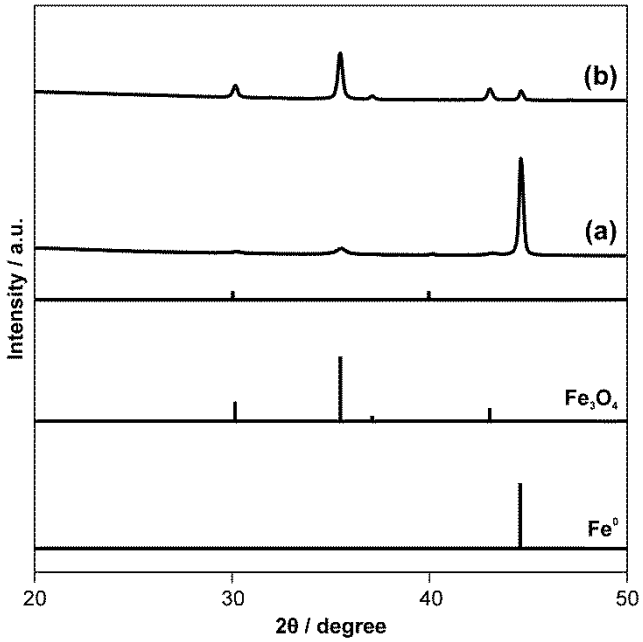

Fig. 4. XRD patterns of Fe samples (a) before and (b) after the transformation reaction.

Diffraction line at 40.3^o is unknown.

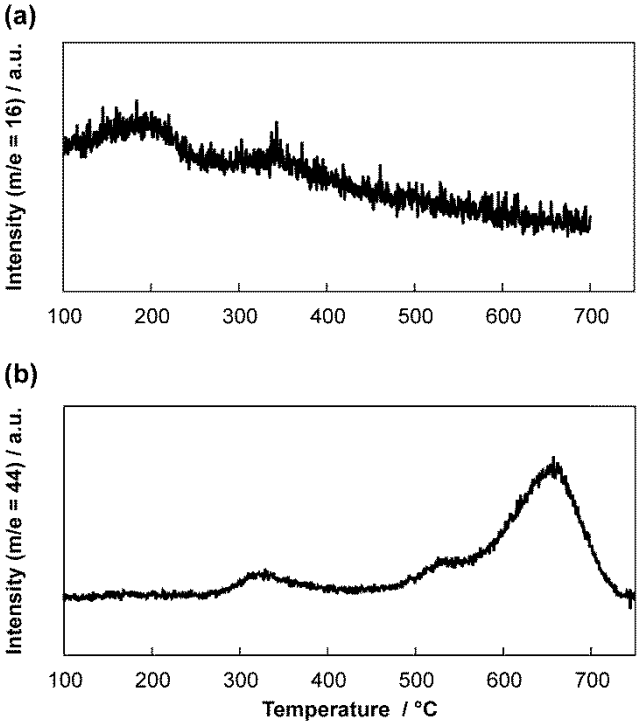

Fig. 5. (a) NH_3- and (b) CO_2-TPD profiles of Fe samples after reaction without Ru–Sn–Mo/C and methyl laurate.

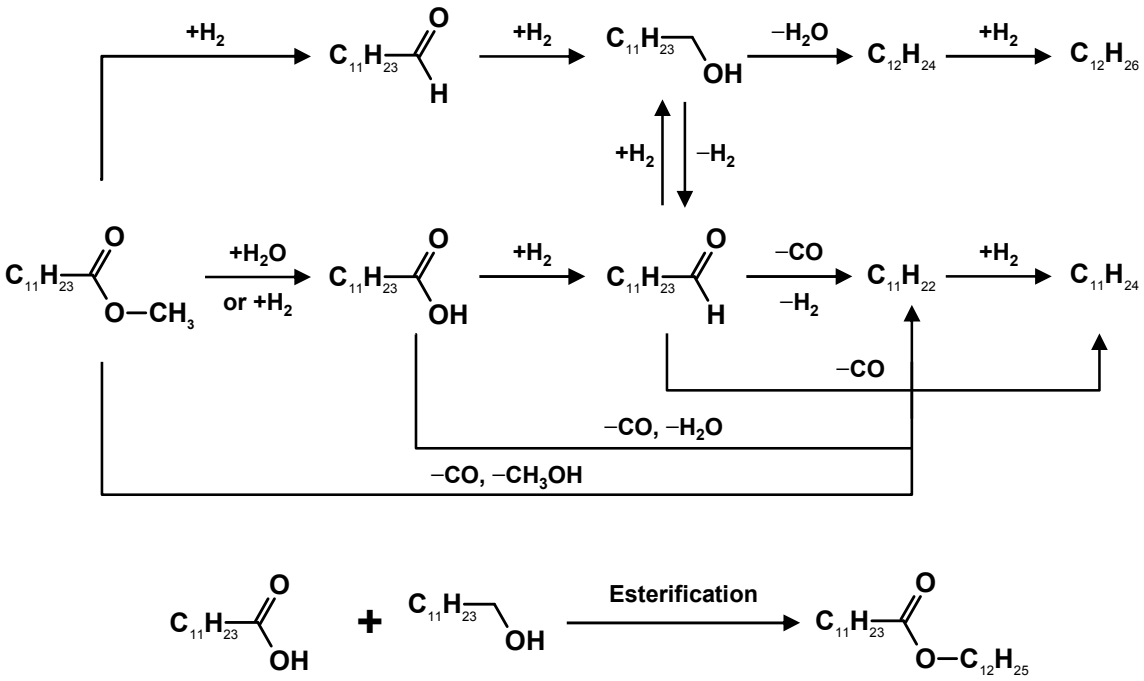

Scheme 1. Reaction pathway for the transformation of methyl laurate based on [61].